



HAL
open science

Critical slope singularities in rotating and stratified fluids

Stéphane Le Dizès

► **To cite this version:**

| Stéphane Le Dizès. Critical slope singularities in rotating and stratified fluids. 2023. hal-04167978v1

HAL Id: hal-04167978

<https://hal.science/hal-04167978v1>

Preprint submitted on 21 Jul 2023 (v1), last revised 31 Oct 2024 (v2)

HAL is a multi-disciplinary open access archive for the deposit and dissemination of scientific research documents, whether they are published or not. The documents may come from teaching and research institutions in France or abroad, or from public or private research centers.

L'archive ouverte pluridisciplinaire **HAL**, est destinée au dépôt et à la diffusion de documents scientifiques de niveau recherche, publiés ou non, émanant des établissements d'enseignement et de recherche français ou étrangers, des laboratoires publics ou privés.

Critical slope singularities in rotating and stratified fluids

Stéphane LE DIZÈS

Aix Marseille Université, CNRS, Centrale Méditerranée, IRPHE, UMR 7342, 13384 Marseille, France

A rotating/stratified fluid supports waves that propagate in directions that depend on their frequency. If the fluid is uniformly rotating around an axis Oz with a rotation rate Ω and/or uniformly stratified along the same axis with a Brünt-Väissälä frequency N , harmonic waves of frequency ω propagate along characteristic lines that make an angle θ with respect to the horizontal plane Oxy with θ satisfying the relation $\omega^2 = 4\Omega^2 \cos^2 \theta + N^2 \sin^2 \theta$. Any infinitesimal oscillation of the boundary is a source of waves but when this boundary is tangent to a direction of propagation of the waves, a singularity generically appears. This critical slope singularity propagates along the critical ray tangent to the boundary. When weak viscous effects are considered, this singular ray forms a concentrated self-similar wave beam with an amplitude that depends on the nature of the singularity and a width of order $(\nu x_{\parallel}/\omega)^{1/3}$, where ν is the kinematic viscosity and x_{\parallel} the distance to the critical point.

The goal of the present work is to provide information on the type of singularities that can be generated in an infinite domain, and therefore on the amplitude and nature of the concentrated wave beams that can be created from critical points. We analyse in a 2D framework two generic configurations corresponding to oscillations normal and tangent to the boundary, respectively. In the first case (oscillations normal to the boundary), we obtain an amplitude scaling in $(\omega r_c^3/(\nu x_{\parallel}))^{1/6}$ corresponding to an inviscid singularity in $x_{\perp}^{-1/2}$, where x_{\perp} is the distance to the critical ray and r_c the curvature radius at the critical point. In the second case (oscillations tangent to the boundary), a weaker beam in $(\nu r_c^3/(\omega x_{\parallel}^5))^{1/12}$ is obtained corresponding to a stronger singularity in $x_{\perp}^{-5/4}$. In that case, the beam is generated by the peculiar viscous boundary layer flow obtained close to the critical point and the problem can be completely solved by a local analysis. A general expression for the beam amplitude is derived that depends on the fluid characteristics (Ω , N), the wave frequency ω , the velocity amplitude of imposed tangential oscillations and the local curvature radius at the critical point. Finally, the first order viscous correction to the critical slope beam induced by the no-slip boundary condition on the surface is also calculated.

I. INTRODUCTION

Waves are ubiquitous in rotating and stratified fluids. In a fluid rotating and uniformly stratified along a same axis Oz , they have the particularity to propagate along characteristic directions making an angle θ with respect to the horizontal plane that only depend on their frequency. When this direction of propagation is tangent to a surface which is potentially a source of waves, a singularity generically appears along this direction. This so-called critical slope singularity is the subject of the present paper.

Figure 1 illustrates the mechanism responsible of the singularity. It shows that if sources were equidistantly placed on the surface of an object, the rays emitted from these sources will tend to accumulate along the characteristic line tangent to the object. The same phenomenon occurs when a plane wave is reflected on a supercritical topography [3].

The footprint of this singularity is clearly visible in experiments. It corresponds to the Saint-Andrews cross that is formed when a small object is oscillated at a frequency in the gravito-inertia wave frequency range [5, 17]. The wave structure obtained from an oscillating cylinder or an oscillating sphere has been extensively studied in the literature [see for instance 1, 8, 9]. The reader is referred to [24, 25] for more references and a comprehensive discussion of the literature.

In the ocean, this singularity is expected to appear when the oscillating tide interacts with a supercritical topography, that is a topography which exhibits a critical slope. This interaction has been studied experimentally [see for instance 27], theoretically [20], and numerically [4].

The structure of the concentrated wave beam associated with this singularity has been the subject of many works in both rotating fluids [10, 14, 16, 26] and stratified fluids [19, 22]. The self-similar expression introduced by [16] and [22] was shown to describe correctly both the far-field of a localized wave source [15, 23], and the intense shear layer emitted from sharp edges [12] and critical slopes [14].

In the present work, we focus on the generic features of the critical slope singularities. Our goal is to provide informations on these singularities and show how they completely govern the structure and strength of the intense shear layers along the critical line.

The paper is organised as follows. In section §II, we first show how the outward radiation condition and the inviscid non-penetration condition on the boundary close to a critical point provide informations on the amplitude and strength of the critical slope singularity. In section §III, we explain how the inviscid singularity is smoothen by

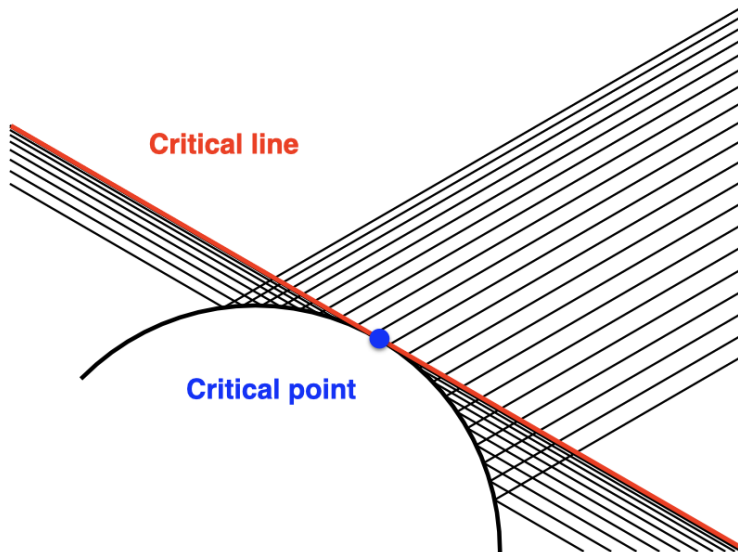


FIG. 1. The rays emitted equidistantly from a surface accumulate on the critical line tangent to the surface at the critical point.

viscosity. The amplitude and structure of the intense shear layer obtained along the critical line is thus provided in this section. Two generic configurations corresponding to a normal and a tangential oscillation of the boundary are then analysed in details in section §IV. The singularity generated by the tangential oscillation is due to the Ekman pumping in the viscous boundary layer. The calculation of this pumping close to a critical point is provided in the appendix. In section §V, we provide the first order viscous correction to the solution derived in section §III. A brief discussion of the results and their possible extension is finally given in the last section §VI.

II. INVISCID ANALYSIS OF CRITICAL SLOPE SINGULARITIES

We consider a weakly viscous incompressible fluid, of kinematic viscosity ν , uniformly rotating around a vertical axis \mathbf{e}_z at the constant rotation rate Ω , and uniformly stratified along the same axis with a constant buoyancy frequency N . The buoyancy diffusivity is neglected and the reference density is fixed to unity.

We are interested in the properties of waves generated by small oscillations of a finite object in infinite domain. The domain and all the fields are assumed to be independent of the spatial variable y such that the analysis can be performed in a fixed plane (Oxz) .

The velocity \mathbf{U} , pressure P , and buoyancy B are assumed to be governed by the Navier-Stokes equations under the Boussinesq approximation

$$\frac{D\mathbf{U}}{Dt} + 2\Omega\mathbf{e}_z \times \mathbf{U} = -\nabla P + B\mathbf{e}_z + \nu\Delta\mathbf{U}, \quad (1a)$$

$$\frac{DB}{Dt} + N^2\mathbf{e}_z \cdot \mathbf{U} = 0, \quad (1b)$$

$$\nabla \cdot \mathbf{U} = 0. \quad (1c)$$

We are interested in linear time-harmonic fluctuations that can be written as

$$(\mathbf{U}, P, B) = (\mathbf{u}, p, b)e^{-i\omega t} + c.c. \quad (2)$$

where *c.c.* denotes the complex conjugate. The amplitudes $\mathbf{u} = (u, v, w)$, p and b satisfy the following system deduced from the linearisation of (1a-c)

$$-i\omega\mathbf{u} + 2\Omega\mathbf{e}_z \times \mathbf{u} = -\nabla p + b\mathbf{e}_z + \nu\Delta\mathbf{u}, \quad (3a)$$

$$-i\omega b + N^2 w = 0, \quad (3b)$$

$$\nabla \cdot \mathbf{u} = 0. \quad (3c)$$

Equation (3c) reads for a velocity field independent of y as $\partial_x u + \partial_z w = 0$. This permits us to introduce a streamfunction $\psi(x, z)$ such that $u = -\partial_z \psi$ and $w = \partial_x \psi$. In an inviscid framework ($\nu = 0$), this function is found to satisfy the so-called Poincaré equation

$$\left[-\omega^2 \left(\frac{\partial^2}{\partial x^2} + \frac{\partial^2}{\partial z^2} \right) + 4\Omega^2 \frac{\partial^2}{\partial z^2} + N^2 \frac{\partial^2}{\partial x^2} \right] \psi = 0. \quad (4)$$

In the presence of rotation ($\Omega \neq 0$), the velocity component v along y is nonzero and given by

$$v = -\frac{2i\Omega}{\omega} u = \frac{2i\Omega}{\omega} \frac{\partial \psi}{\partial z}. \quad (5)$$

Similarly, in the presence of stratification ($N \neq 0$), there is a buoyancy perturbation given by

$$b = -\frac{iN^2}{\omega} w = -\frac{iN^2}{\omega} \frac{\partial \psi}{\partial x}. \quad (6)$$

We shall assume that the frequency ω is between N and 2Ω . In that case, equation (4) is an homogeneous hyperbolic equation whose characteristics are the lines that makes an angle θ with respect to the horizontal plane given by

$$\omega^2 = 4\Omega^2 \cos^2 \theta + N^2 \sin^2 \theta. \quad (7)$$

We can assume that $0 \leq \theta \leq \pi/2$. The three other solutions of (7) are $-\theta$, $\pi + \theta$ and $\pi - \theta$. In the following, we shall denote the three directions θ , $\pi - \theta$, and $-\theta$ by NE (North-East), NW (North-West) and SE (South-East).

It is useful to introduce a coordinate system connected to the characteristics. We define the variables x_{\perp}^{NE} and $x_{\parallel}^{\text{NE}}$ (resp. x_{\perp}^{NW} and $x_{\parallel}^{\text{NW}}$) along the vectors $\mathbf{e}_{\perp}^{\text{NE}}$ and $\mathbf{e}_{\parallel}^{\text{NE}}$ (resp. $\mathbf{e}_{\perp}^{\text{NW}}$ and $\mathbf{e}_{\parallel}^{\text{NW}}$) for the wave propagating in the NE direction (resp NW direction):

$$x_{\perp}^{\text{NE}} = -\sin \theta x + \cos \theta z, x_{\parallel}^{\text{NE}} = \cos \theta x + \sin \theta z, \quad (8a)$$

$$x_{\perp}^{\text{NW}} = \sin \theta x + \cos \theta z, x_{\parallel}^{\text{NW}} = -\cos \theta x + \sin \theta z, \quad (8b)$$

Equation (4) can then be written as

$$\frac{\partial}{\partial x_{\perp}^{\text{NE}}} \frac{\partial}{\partial x_{\perp}^{\text{NW}}} \psi = 0, \quad (9)$$

so its general solution can be written as

$$\psi(x, z) = F(x_{\perp}^{\text{NE}}) + G(x_{\perp}^{\text{NW}}), \quad (10)$$

where F and G are two arbitrary functions. The velocity field \mathbf{u}_{2D} (in the (x, z) plane) reads

$$\mathbf{u}_{2D} = F'(x_{\perp}^{\text{NE}})\mathbf{e}_{\parallel}^{\text{NE}} + G'(x_{\perp}^{\text{NW}})\mathbf{e}_{\parallel}^{\text{NW}}. \quad (11)$$

In general, G describes waves propagating in both $\mathbf{e}_{\parallel}^{\text{NW}}$ and $\mathbf{e}_{\parallel}^{\text{SE}} = -\mathbf{e}_{\parallel}^{\text{NW}}$. The part that is propagating in a given direction is obtained by splitting the Fourier decomposition of G into positive and negative wavenumbers:

$$G(x_{\perp}^{\text{NW}}) = \int_0^{+\infty} \hat{G}(k) e^{ikx_{\perp}^{\text{NW}}} dk + \int_{-\infty}^0 \hat{G}(k) e^{ikx_{\perp}^{\text{NW}}} dk. \quad (12)$$

The first part, associated with positive k , describes a wavepacket with phase velocities oriented along $\mathbf{e}_{\perp}^{\text{NW}}$ (assuming $\omega > 0$). The group velocity of this wavepacket, that gives the direction of propagation, is oriented along with $\mathbf{e}_{\parallel}^{\text{NW}}$ if

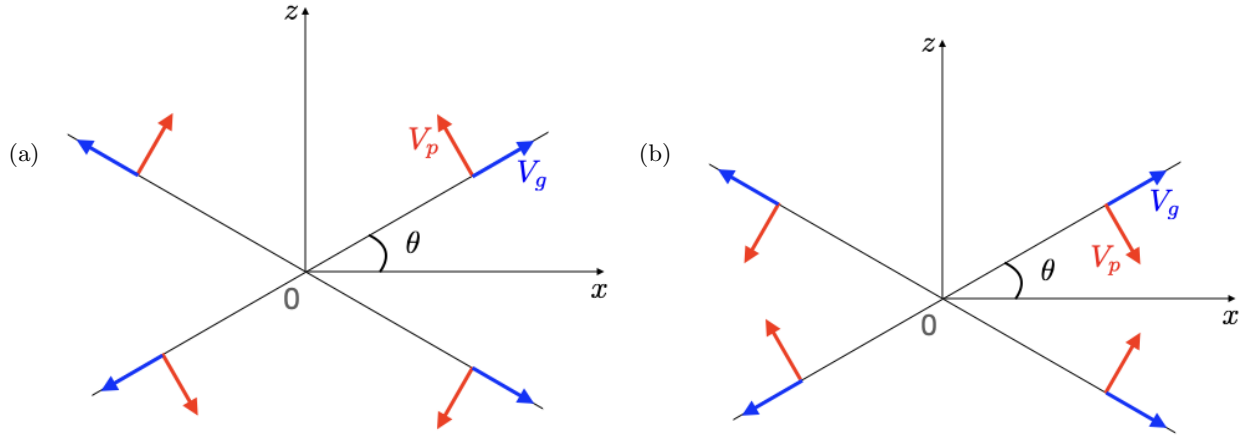


FIG. 2. Relation between phase velocity and group velocity orientations. (a) $N < 2\Omega$, (b) $2\Omega < N$.

$N < 2\Omega$, but with $-\mathbf{e}_{\parallel}^{\text{NW}}$ if $N > 2\Omega$ (see figure 2). This means, that if $N < 2\Omega$, the wavepacket composed of positive wavenumbers propagates in the direction of $\mathbf{e}_{\parallel}^{\text{NE}}$ and the one of negative wavenumbers in the direction $-\mathbf{e}_{\parallel}^{\text{NW}}$. It is the opposite if $N > 2\Omega$.

As explained by [2], the condition of causality can be directly expressed as a condition on the functions F and G . For instance, the function G defines a wave packet that propagates in the direction $+\theta$ if

$$G(x_{\perp}^{\text{NW}}) = -\frac{i\epsilon}{\pi} P \int_{-\infty}^{\infty} \frac{G(\eta)}{\eta - x_{\perp}^{\text{NW}}} d\eta, \quad (13)$$

where the P in front of the integral means that the Cauchy Principal Part of the integral is taken. The wave packet propagating in the opposite direction $\pi + \theta$ satisfies

$$G(x_{\perp}^{\text{NW}}) = \frac{i\epsilon}{\pi} P \int_{-\infty}^{\infty} \frac{F(\eta)}{\eta - x_{\perp}^{\text{NW}}} d\eta. \quad (14)$$

In these equations, $\epsilon = \text{sgn}(2\Omega - N)$. When $\epsilon = -1$, we recover the conditions obtained by Baines for the non-rotating case.

We shall be interested in solutions exhibiting singularities along the line $x_{\perp}^{\text{NE}} = 0$ or $x_{\perp}^{\text{NW}} = 0$ issued from the critical point at $(x_{\perp}^{\text{NE}}, x_{\perp}^{\text{NW}}) = (0, 0)$. The nature of this singularity is subject to constraints that come from the condition of radiation. If $G(x_{\perp}^{\text{NW}})$ exhibits the following behaviors close to $x_{\perp}^{\text{NW}} = 0$:

$$G(x_{\perp}^{\text{NW}}) \sim \frac{C^+}{(x_{\perp}^{\text{NW}})^{\alpha}}, \quad x_{\perp}^{\text{NW}} > 0, \quad (15a)$$

$$G(x_{\perp}^{\text{NW}}) \sim \frac{C^-}{(-x_{\perp}^{\text{NW}})^{\alpha}}, \quad x_{\perp}^{\text{NW}} < 0, \quad (15b)$$

there is a relation between C^+ and C^- if it also satisfies (13):

$$C^+ = e^{i\pi\alpha\epsilon} C^-. \quad (16)$$

The relation is

$$C^+ = e^{-i\pi\alpha\epsilon} C^-, \quad (17)$$

if it satisfies (14) instead of (13).

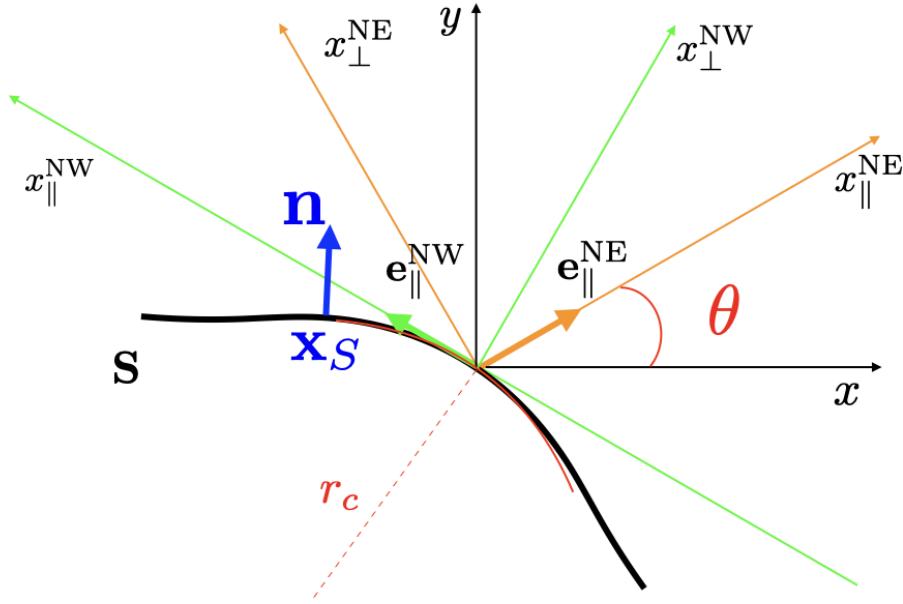


FIG. 3. Coordinate system near a critical point. One of the direction of propagation is tangent to the surface boundary.

These relations directly come from the equalities

$$\frac{i}{\pi} P \int_0^{\infty} \frac{d\eta}{(\eta-x)\eta^\alpha} = \begin{cases} \frac{i \cos(\pi\alpha)}{\sin(\pi\alpha)x^\alpha} & x > 0, \\ \frac{i}{\sin(\pi\alpha)(-x)^\alpha} & x < 0, \end{cases} \quad (18a)$$

$$\frac{i}{\pi} P \int_{-\infty}^0 \frac{d\eta}{(\eta-x)(-\eta)^\alpha} = \begin{cases} -\frac{i}{\sin(\pi\alpha)x^\alpha} & x > 0, \\ -\frac{i \cos(\pi\alpha)}{\sin(\pi\alpha)(-x)^\alpha} & x < 0, \end{cases} \quad (18b)$$

obtained for $0 < \alpha < 1$.

If $\alpha \leq 0$, $G(x_\perp^{\text{NW}})$ vanishes or is finite at $x_\perp^{\text{NW}} = 0$. In that case, an estimate of the integral in the right-hand side of (13) cannot be obtained using the local behavior of G close to 0. However, if α is not a negative integer, one just has to differentiate G once or several times such that its derivative satisfies (15a,b) with a value of α between 0 and 1. Similarly, if $\alpha > 1$, the integral on the RHS of (13) does not converge, so this equation cannot be used. However, as above, if α is not a positive integer, one can integrate G once (or several times) such that the primitive of G is less singular, and satisfies (15a,b) with $0 < \alpha < 1$. For both cases, one can then use the relation (16) for the coefficients of either derivatives or primitives of G . Since differentiation and integration just change α by an integer, (16) is thus valid for any α provided α is not an integer. Finally, note that if $\alpha = 0$, (16) would prescribe no jump, that is no singularity.

We assume that the waves are generated from the displacement of the boundaries. In an inviscid framework, at any point \mathbf{x}_S of the boundary S , the velocity field amplitude \mathbf{u} should satisfy the non-penetrability condition

$$\mathbf{u}(\mathbf{x}_S) \cdot \mathbf{n}(\mathbf{x}_S) = U_{0n}(\mathbf{x}_S), \quad (19)$$

where $U_{0n}(\mathbf{x}_S)$ and $\mathbf{n}(\mathbf{x}_S)$ are the normal velocity amplitude and normal vector of the boundary at \mathbf{x}_S .

We are looking for solutions close to a critical point and choose the origin of the frame at the critical point. The geometry of the problem can then generically be sketched as shown in figure 3. The critical line, tangent to the surface at the origin is given by the equation $x_\perp^{\text{NW}} = 0$. The line $x_\perp^{\text{NE}} = 0$ divide the domain into two regions.

Close to the critical point, the surface S can be defined in terms of the variables x_\perp^{NE} and x_\perp^{NW} by

$$x_\perp^{\text{NW}} \sim -\frac{(x_\perp^{\text{NE}})^2}{2r_c(\sin 2\theta)^2} \quad \text{for } x_\perp^{\text{NW}} < 0, \quad (20)$$

or

$$x_{\perp}^{\text{NE}} \sim \sqrt{2r_c|x_{\perp}^{\text{NW}}|} \sin 2\theta \quad \text{for } x_{\perp}^{\text{NE}} > 0, x_{\perp}^{\text{NW}} < 0, \quad (21a)$$

$$x_{\perp}^{\text{NE}} \sim -\sqrt{2r_c|x_{\perp}^{\text{NW}}|} \sin 2\theta \quad \text{for } x_{\perp}^{\text{NE}} < 0, x_{\perp}^{\text{NW}} < 0. \quad (21b)$$

where r_c is the radius of curvature at the critical point.

Similarly, close to the critical point, we can express the cartesian components of $\mathbf{n}(\mathbf{x}_S)$ in terms of x_{\perp}^{NE}

$$n_x(\mathbf{x}_S) \sim \sin \theta - \frac{x_{\perp}^{\text{NE}}}{2r_c \sin \theta}, \quad (22)$$

$$n_z(\mathbf{x}_S) \sim \cos \theta + \frac{x_{\perp}^{\text{NE}}}{2r_c \cos \theta}.$$

If the velocity field \mathbf{U} is expressed in terms of the streamfunction ψ defined in (10), $\mathbf{U} \cdot \mathbf{n}$ can then be written close to the critical point as

$$\mathbf{U}(\mathbf{x}_S) \cdot \mathbf{n}(\mathbf{x}_S) \sim \sin 2\theta F'(x_{\perp}^{\text{NE}}) + \frac{x_{\perp}^{\text{NE}}}{r_c \sin 2\theta} G'(x_{\perp}^{\text{NW}}). \quad (23)$$

As the relation between x_{\perp}^{NE} and x_{\perp}^{NW} depends on the sign of x_{\perp}^{NE} , we expect two expressions for ψ :

$$\psi_+ = F(x_{\perp}^{\text{NE}}) + G_+(x_{\perp}^{\text{NW}}) \quad \text{for } x_{\perp}^{\text{NE}} > 0, \quad (24a)$$

$$\psi_- = F(x_{\perp}^{\text{NE}}) + G_-(x_{\perp}^{\text{NW}}) \quad \text{for } x_{\perp}^{\text{NE}} < 0. \quad (24b)$$

The condition (19) implies that close to the critical point for $x_{\perp}^{\text{NW}} < 0$

$$\sin 2\theta F'(x_{\perp}^{\text{NE}}) + \sqrt{\frac{2|x_{\perp}^{\text{NW}}|}{r_c}} G'_+(x_{\perp}^{\text{NW}}) \sim U_{0n}(\mathbf{x}_S) \quad (25a)$$

$$\text{with } x_{\perp}^{\text{NE}} \sim \sqrt{2r_c|x_{\perp}^{\text{NW}}|} \sin 2\theta, \quad \text{when } x_{\perp}^{\text{NE}} > 0,$$

$$\sin 2\theta F'(x_{\perp}^{\text{NE}}) - \sqrt{\frac{2|x_{\perp}^{\text{NW}}|}{r_c}} G'_-(x_{\perp}^{\text{NW}}) \sim U_{0n}(\mathbf{x}_S) \quad (25b)$$

$$\text{with } x_{\perp}^{\text{NE}} \sim -\sqrt{2r_c|x_{\perp}^{\text{NW}}|} \sin 2\theta, \quad \text{when } x_{\perp}^{\text{NE}} < 0.$$

The function F defines a wavepacket propagating towards the North-East direction. This condition is written as

$$F'(x_{\perp}^{\text{NE}}) = -\epsilon \frac{i}{\pi} P \int_{-\infty}^{\infty} \frac{F'(\eta)}{\eta - x_{\perp}^{\text{NE}}} d\eta, \quad (26)$$

where $\epsilon = \text{sign}(2\Omega - N)$.

Similarly, the function G_+ and the function G_- define wavepackets propagating towards the North-West direction and towards the South-East direction, respectively. The function G_+ must then satisfy (13) while G_- must satisfy (14):

$$G'_+(x_{\perp}^{\text{NW}}) = -\epsilon \frac{i}{\pi} P \int_{-\infty}^{\infty} \frac{G'_+(\eta)}{\eta - x_{\perp}^{\text{NW}}} d\eta, \quad (27a)$$

$$G'_-(x_{\perp}^{\text{NW}}) = \epsilon \frac{i}{\pi} P \int_{-\infty}^{\infty} \frac{G'_-(\eta)}{\eta - x_{\perp}^{\text{NW}}} d\eta. \quad (27b)$$

Moreover, for $x_{\perp}^{\text{NW}} > 0$, G_+ and G_- define a same function and therefore one should have

$$G_+(x_{\perp}^{\text{NW}}) = G_-(x_{\perp}^{\text{NW}}) \quad \text{for } x_{\perp}^{\text{NW}} > 0. \quad (28)$$

We can now look at the compatibility of these equations for singular fields. Assume for instance that $U_n(\mathbf{x}_S)$ behaves as

$$U_{0n}(\mathbf{x}_S) \sim \frac{C_+}{(x_{\perp}^{\text{NE}})^{\beta}} \quad \text{for } x_{\perp}^{\text{NE}} > 0, \quad (29a)$$

$$U_{0n}(\mathbf{x}_S) \sim \frac{C_-}{(-x_{\perp}^{\text{NE}})^{\beta}} \quad \text{for } x_{\perp}^{\text{NE}} < 0. \quad (29b)$$

The boundary conditions (25a,b) indicate that $F'(x_{\perp}^{\text{NE}})$ and $G'_{\pm}(x_{\perp}^{\text{NW}})$ should behave for small values of their variable as

$$F'(x_{\perp}^{\text{NE}}) \sim \frac{D_+}{(x_{\perp}^{\text{NE}})^{\beta}} \quad \text{for } x_{\perp}^{\text{NE}} > 0, \quad (30a)$$

$$F'(x_{\perp}^{\text{NE}}) \sim \frac{D_-}{(-x_{\perp}^{\text{NE}})^{\beta}} \quad \text{for } x_{\perp}^{\text{NE}} < 0. \quad (30b)$$

and

$$G'_+(x_{\perp}^{\text{NW}}) \sim \frac{E_+}{(-x_{\perp}^{\text{NW}})^{(\beta+1)/2}} \quad \text{for } x_{\perp}^{\text{NW}} < 0, \quad (31a)$$

$$G'_-(x_{\perp}^{\text{NW}}) \sim \frac{E_-}{(-x_{\perp}^{\text{NW}})^{(\beta+1)/2}} \quad \text{for } x_{\perp}^{\text{NW}} < 0. \quad (31b)$$

We also expect for $x_{\perp}^{\text{NW}} > 0$ a behavior of $G_+ = G_- = G$ of same nature:

$$G'(x_{\perp}^{\text{NW}}) \sim \frac{E_o}{(x_{\perp}^{\text{NW}})^{(\beta+1)/2}} \quad \text{for } x_{\perp}^{\text{NW}} > 0. \quad (32)$$

As explained above, the condition that each wave is an outward wave implies conditions on the coefficients D_{\pm} , E_{\pm} and E_o that can be written as

$$D_+ = e^{i\epsilon\pi\beta} D_-, \quad (33a)$$

$$E_o = i\epsilon e^{i\epsilon\pi\beta/2} E_+, \quad (33b)$$

$$E_o = -i\epsilon e^{-i\epsilon\pi\beta/2} E_-. \quad (33c)$$

The last two equations means that

$$E_+ = -e^{-i\epsilon\pi\beta} E_-. \quad (34)$$

One can now write down the conditions obtained from (25a,b):

$$\sin 2\theta D_+ + \sqrt{\frac{2}{r_c}} (\sqrt{2r_c} \sin 2\theta)^{\beta} E_+ = C_+, \quad (35a)$$

$$\sin 2\theta D_- - \sqrt{\frac{2}{r_c}} (\sqrt{2r_c} \sin 2\theta)^{\beta} E_- = C_-. \quad (35b)$$

The system of equations (33a), (34) and (35a-b) is a linear non-homogeneous system for E_+ , E_- , D_+ and D_- . It admits a unique solution whatever C_+ and C_- if and only if

$$e^{2i\pi\beta} \neq 1, \quad (36)$$

that is β is not an integer. This condition was already required to derive equations (33a-c).

In that case, this unique solution is given by

$$D_+ = \epsilon \frac{e^{i\epsilon\pi\beta} C_+ - C_-}{2i \sin \pi\beta \sin 2\theta}, \quad (37a)$$

$$D_- = \epsilon \frac{C_+ - e^{-i\epsilon\pi\beta} C_-}{2i \sin \pi\beta \sin 2\theta}, \quad (37b)$$

$$E_+ = \epsilon \frac{C_- - e^{-i\epsilon\pi\beta} C_+}{2i (\sqrt{2r_c} \sin 2\theta)^{\beta} \sin \pi\beta} \sqrt{\frac{r_c}{2}}, \quad (37c)$$

$$E_- = \epsilon \frac{C_+ - e^{i\epsilon\pi\beta} C_-}{2i (\sqrt{2r_c} \sin 2\theta)^{\beta} \sin \pi\beta} \sqrt{\frac{r_c}{2}}, \quad (37d)$$

$$E_o = \frac{e^{i\epsilon\pi\beta/2} C_- - e^{-i\epsilon\pi\beta/2} C_+}{2 (\sqrt{2r_c} \sin 2\theta)^{\beta} \sin \pi\beta} \sqrt{\frac{r_c}{2}}. \quad (37e)$$

It only depends on the angle θ , the curvature radius of the boundary at the critical point and on the behaviour of $U_n(\mathbf{x}_s)$ close to the critical point via the coefficients C_+ , C_- and the singularity exponent β .

When $\beta = 0$, the above analysis has to be modified. Since (25a,b) still apply, one can expect a singularity of G' in $(-x_{\perp}^{\text{NW}})^{-1/2}$ but F' should remain regular and simply given by a constant $F'(0)$. This means that we should still have (30a,b), (31a,b), (32) with (33a-c) for $\beta = 0$. The system (35a,b) obtained for $\beta = 0$ is then still valid. It admits a solution only if $C_+ = C_- = U_{0n}(0)$. This solution is

$$E_+ = (U_{0n}(0) - \sin 2\theta F'(0)) \sqrt{\frac{r_c}{2}}, \quad (38a)$$

$$E_- = -E_+, \quad (38b)$$

$$E_o = i\epsilon E_+, \quad (38c)$$

$$D_+ = D_- = F'(0). \quad (38d)$$

It depends on an undetermined constant $F'(0)$ which is the amplitude of the velocity of the wavepacket emitted in the direction $\mathbf{e}_{\parallel}^{\text{NE}}$ on the critical ray (see expression (11)).

III. VISCOUS SMOOTHING OF THE CRITICAL SLOPE SINGULARITY

In a real fluid, diffusion or viscosity is expected to smooth inviscid singularities. A similar phenomenon is active for the singularities that are created from critical slopes.

We have seen that the singular inviscid solution that propagates in the North-West direction can be written as (for $x_{\perp}^{\text{NE}} > 0$)

$$u_{\parallel}^{\text{NW}} \sim \frac{E_o}{(x_{\perp}^{\text{NW}})^{\mu}} \quad \text{for } x_{\perp}^{\text{NW}} > 0, \quad (39a)$$

$$u_{\parallel}^{\text{NW}} \sim \frac{E_o e^{-i\epsilon\pi\mu}}{(-x_{\perp}^{\text{NW}})^{\mu}} \quad \text{for } x_{\perp}^{\text{NW}} < 0. \quad (39b)$$

The viscous smoothing of a singularity of this form has already been studied by [16] for rotating fluids and [22] for stratified fluids. An expression valid for a general rotating and stratified fluid has been given in [13]. For a 2D configuration without buoyancy diffusion (infinite Prandtl number), this expression reads as

$$u_{\parallel}^{\text{NW}} \sim C^{\text{NW}} \mathbf{H}_{\mu}(\zeta^{\text{NW}}, x_{\parallel}^{\text{NW}}) = C^{\text{NW}} \frac{h_{\mu}(\zeta^{\text{NW}})}{(x_{\parallel}^{\text{NW}})^{\mu/3}}, \quad (40)$$

where ζ^{NW} is the self-similar variable

$$\zeta^{\text{NW}} = \epsilon \frac{x_{\perp}^{\text{NW}}}{(x_{\parallel}^{\text{NW}} \Lambda \nu / \omega)^{1/3}}, \quad (41)$$

with

$$\Lambda = \frac{2\gamma^2 \cos^2 \theta + \sin^2 \theta}{\sin 2\theta |\gamma^2 - 1|}, \quad \gamma = 2\Omega/N, \quad (42)$$

and $h_{\mu}(\zeta)$ is the Moore-Saffman Thomas-Stevenson function

$$h_{\mu}(\zeta) = \frac{e^{-i\mu\pi/2}}{(\mu-1)!} \int_0^{+\infty} e^{ip\zeta - p^3} p^{\mu-1} dp, \quad (43)$$

defined for $\mu > 0$. The function $h_{\mu}(\zeta)$ satisfies [see 16]

$$h_{\mu}(\zeta) \sim \frac{1}{|\zeta|^{\mu}} \quad \text{as } \zeta \rightarrow +\infty, \quad (44a)$$

$$h_{\mu}(\zeta) \sim \frac{e^{-i\mu\pi}}{|\zeta|^{\mu}} \quad \text{as } \zeta \rightarrow -\infty. \quad (44b)$$

A simple matching of (40) with (39a,b) then gives

$$C^{\text{NW}} = \left(\frac{\omega}{\nu\Lambda}\right)^{\mu/3} e^{i\frac{\pi}{2}\mu(1-\epsilon)} E_o. \quad (45)$$

Expression (40) with (41) and (45) describes a localized beam of width $(x_{\parallel}^{\text{NW}}\Lambda\nu/\omega)^{1/3}$ and velocity amplitude $(\omega/(\nu\Lambda x_{\parallel}^{\text{NW}}))^{\mu/3}E_o$. Note in particular that the beam becomes wider and weaker as we get away from the critical point.

A similar analysis can be done for the beam propagating in the South-East direction. If we define $\mathbf{e}_{\parallel}^{\text{SE}} = -\mathbf{e}_{\parallel}^{\text{NW}}$ and $\mathbf{e}_{\perp}^{\text{SE}} = -\mathbf{e}_{\perp}^{\text{NW}}$, the inviscid solution propagating in the SE direction that agrees with (39) is

$$u_{\parallel}^{\text{SE}} \sim \frac{-E_o e^{i\epsilon\pi\mu}}{(x_{\perp}^{\text{SE}})^{\mu}} \quad \text{for } x_{\perp}^{\text{SE}} > 0, \quad (46a)$$

$$u_{\parallel}^{\text{SE}} \sim \frac{-E_o}{(-x_{\perp}^{\text{SE}})^{\mu}} \quad \text{for } x_{\perp}^{\text{SE}} < 0. \quad (46b)$$

We then immediately obtain

$$u_{\parallel}^{\text{SE}} \sim C^{\text{SE}} H_{\mu}(\zeta^{\text{SE}}, x_{\parallel}^{\text{SE}}), \quad (47)$$

with $C^{\text{SE}} = -e^{i\epsilon\mu\pi} C^{\text{NW}}$.

It is worth mentioning that the above analysis is valid only if the non-viscous approximation (39a,b) applies when $x_{\perp} \gg (x_{\parallel}\Lambda\nu/\omega)^{1/3}$ close to the critical point. This property is satisfied for the beams propagating in the NW and SE directions because the width of the viscous boundary layer remains of order $\nu^{2/5}$ (which corresponds to $x_{\perp}^{\text{NW}} = O(\nu^{2/5})$) at a distance $x_{\parallel}^{\text{NW}} = O(\nu^{1/5})$ from the critical point [10, 11, 21].

By contrast, for the beam propagating in the NE direction, viscous effects are expected to appear close to the critical point as soon as $x_{\perp}^{\text{NE}} = O(\nu^{1/5})$. The beam propagating in that direction is possibly larger and not described by the similarity solution.

IV. APPLICATIONS

A. Normal displacement

This situation corresponds to a generic configuration where the object is displaced in translation or subjected to an external oscillating flow. In the linear regime, these two configurations are equivalent. What is important is the normal velocity of the object boundary close to the critical point with respect to the fluid. When there is a normal displacement, this velocity is nonzero and given by the projection of the boundary velocity along the normal vector at the critical point:

$$U_{0n}(\mathbf{x}_{S_c}) = \mathbf{U}_b \cdot \mathbf{n}(\mathbf{x}_{S_c}) = U_b \sin \theta + V_b \cos \theta, \quad (48)$$

if $\mathbf{U}_b = (U_b, V_b)$ is the velocity in the (x, z) plane of the object boundary with respect to the fluid. The normal velocity is therefore not singular and given by expression (29a,b) with $\beta = 0$ and $C_+ = C_- = U_{0n}(\mathbf{x}_{S_c})$.

The nature of the singularity along the critical line is therefore expected to be always of same nature with a velocity diverging as $(x_{\perp}^{\text{NW}})^{-1/2}$. However, its amplitude cannot be obtained in closed form. It depends on the velocity along the line $x_{\perp}^{\text{NE}} = 0$ from the critical point, that is the constant $F'(0)$. As shown above, the velocity close to the critical line $x_{\perp}^{\text{NW}} = 0$ is given by

$$\mathbf{u} \sim G'(x_{\perp}^{\text{NW}}) \mathbf{e}_{\parallel}^{\text{NW}}, \quad (49)$$

where

$$G'(x_{\perp}^{\text{NW}}) \sim \begin{cases} E_+ (-x_{\perp}^{\text{NW}})^{-1/2} & \text{for } x_{\perp}^{\text{NW}} < 0; \quad x_{\perp}^{\text{NE}} > 0 \\ -E_+ (-x_{\perp}^{\text{NW}})^{-1/2} & \text{for } x_{\perp}^{\text{NW}} < 0; \quad x_{\perp}^{\text{NE}} < 0 \\ i\epsilon E_+ (x_{\perp}^{\text{NW}})^{1/2} & \text{for } x_{\perp}^{\text{NW}} > 0 \end{cases} \quad (50)$$

with

$$E_+ = (U_b \sin \theta + V_b \cos \theta - \sin 2\theta F'(0)) \sqrt{r_c/2}. \quad (51)$$

As an illustration, one can look at the flow generated by an oscillating circular cylinder in a non-rotating fluid. The general solution has been provided by [8] for an elliptic cylinder. For a circular cylinder of radius r_c , the solution reads as

$$\mathbf{u} = \frac{\partial\psi}{\partial\sigma_+} \mathbf{e}_{\parallel}^{\text{NE}} + \frac{\partial\psi}{\partial\sigma_-} \mathbf{e}_{\parallel}^{\text{NW}}, \quad (52)$$

with

$$\frac{\partial\psi}{\partial\sigma_{\pm}} = \alpha_{\pm} \left(1 - \frac{\sigma_{\pm}}{\sqrt{\sigma_{\pm}^2 - r_c^2}} \right), \quad (53)$$

where the constants α_{\pm} are given by

$$\alpha_{\pm} = \frac{1}{2} (iV_b \pm U_b) e^{-i\theta}, \quad (54)$$

and the coordinates σ_{\pm} are related to our coordinates x_{\perp}^{NE} and x_{\perp}^{NW} by

$$\sigma_+ = -x_{\perp}^{\text{NE}} - r_c \cos(2\theta), \quad (55)$$

$$\sigma_- = x_{\perp}^{\text{NW}} + r_c. \quad (56)$$

The definition of the square root depends on the position with respect to the critical lines $\sigma_+ = \pm r_c$ and $\sigma_- = \pm r_c$. We get close to the critical point $(x_{\perp}^{\text{NE}}, x_{\perp}^{\text{NW}}) = (0, 0)$

$$\frac{\partial\psi}{\partial\sigma_+} \sim \alpha_+ (1 - i \cot(2\theta)) = \frac{(V_b - iU_b) e^{i\theta}}{2 \sin 2\theta} = F'(0), \quad (57)$$

and

$$\frac{\partial\psi}{\partial\sigma_-} \sim \begin{cases} -i\sqrt{\frac{r_c}{2}} \alpha_- (-x_{\perp}^{\text{NW}})^{-1/2} & \text{for } x_{\perp}^{\text{NW}} < 0, x_{\perp}^{\text{NE}} > 0, \\ i\sqrt{\frac{r_c}{2}} \alpha_- (-x_{\perp}^{\text{NW}})^{-1/2} & \text{for } x_{\perp}^{\text{NW}} < 0, x_{\perp}^{\text{NE}} < 0, \\ -\sqrt{\frac{r_c}{2}} \alpha_- (x_{\perp}^{\text{NW}})^{-1/2} & \text{for } x_{\perp}^{\text{NW}} > 0, \end{cases} \quad (58)$$

which is in agreement with formulas (50) for the non-rotating case ($\epsilon = -1$) if one uses (57) for $F'(0)$ in E_+ and (54) for α_- .

As explained above, from the inviscid solution close to the singularity, one can immediately get the viscous solution smoothing the singularity. Here it gives along the NW and SE directions

$$u_{\parallel}^{\text{NW}} \sim e^{i\frac{\pi}{4}(1+\epsilon)} E_+ \left(\frac{\omega}{\nu\Lambda} \right)^{1/6} \text{H}_{1/2}(\zeta^{\text{NW}}, x_{\parallel}^{\text{NW}}), \quad (59a)$$

$$u_{\parallel}^{\text{SE}} \sim e^{i\frac{\pi}{4}(1-\epsilon)} E_+ \left(\frac{\omega}{\nu\Lambda} \right)^{1/6} \text{H}_{1/2}(\zeta^{\text{SE}}, x_{\parallel}^{\text{SE}}), \quad (59b)$$

where the function H_{μ} has been defined in (40-43), and E_+ is given by (51). These expressions show that the velocity field generated by a normal displacement is $O(\nu^{-1/6})$ larger near the critical line than the forcing amplitude. The amplitude nevertheless decreases as $x_{\parallel}^{-1/6}$ with the distance x_{\parallel} from the critical point.

B. Tangential displacement

When the surface displacement is tangent to the surface, there is no inviscid forcing. The forcing of the wave is due in that case to the Ekman pumping generated by viscous effects close to the boundary. The normal velocity $u_{n\infty}$ associated with this Ekman pumping is calculated in the appendix A for a general tangential displacement $U_S \mathbf{e}_t + V_S \mathbf{e}_y$ of the boundary. It is this velocity component that provides the forcing term $U_{0n}(\mathbf{x}_S) = u_{n\infty}$ of the waves where $u_{n\infty}$ is given by (A18). Close to a critical point, the Ekman pumping exhibits a singular behavior which can be written in terms of the variable x_{\perp}^{NE} using

$$x_{\perp}^{\text{NE}} \sim -\sin 2\theta \alpha_c (s - s_c) \quad (60)$$

as

$$u_{n\infty} \sim \mp \sqrt{\frac{\nu r_c}{\omega}} \frac{e^{\mp i\pi/4} (\sin 2\theta)^{3/2}}{|x_{\perp}^{\text{NE}}|^{3/2}} (\bar{F}_u(\theta, 2\Omega/N) U_S + i\bar{F}_v(\theta, 2\Omega/N) V_S). \quad (61)$$

where

$$\bar{F}_u(\theta, \gamma) = \frac{\gamma^2 \cos^2 \theta + \sin^2 \theta}{2 (\sin 2\theta (2\gamma^2 \cos^2 \theta + \sin^2 \theta) |\gamma^2 - 1|)^{1/2}}, \quad (62a)$$

$$\bar{F}_v(\theta, \gamma) = \frac{\gamma \cos \theta}{2} \left(\frac{\gamma^2 \cos^2 \theta + \sin^2 \theta}{\sin 2\theta (2\gamma^2 \cos^2 \theta + \sin^2 \theta) |\gamma^2 - 1|} \right)^{1/2}. \quad (62b)$$

The normal velocity is therefore of the form (29) with $\beta = 3/2$ and

$$C^+ = e^{i\epsilon\pi/2} C^- = -e^{-i\epsilon\pi/4} \sqrt{\frac{\nu r_c}{\omega}} (\sin 2\theta)^{3/2} (\bar{F}_u U_S + i\bar{F}_v V_S). \quad (63)$$

Applying formulas (37a-e) gives

$$D_+ = D_- = 0, \quad (64a)$$

$$E_o = -e^{i\epsilon\pi/4} E_+ = -e^{-i\epsilon\pi/2} E_- = \sqrt{\frac{\nu}{\omega}} \frac{r_c^{1/4}}{2^{5/4}} (\bar{F}_u U_S + i\bar{F}_v V_S). \quad (64b)$$

A tangential displacement of the boundary then gives rise to a critical slope singularity in $|x_{\perp}^{\text{NW}}|^{-5/4}$ with an amplitude of order $\nu^{1/2}$.

As explained above, such a singularity, when smoothed by viscous/diffusion effect produces a thin internal shear layer that can be described by the Moore-Saffman / Thomas-Stevenson self-similar solution. The north-west and south-east critical slope beams are then given by

$$u_{\parallel}^{\text{NW}} \sim C_0^{\text{NW}} \text{H}_{5/4}(\zeta^{\text{NW}}, x_{\parallel}^{\text{NW}}), \quad (65a)$$

$$u_{\parallel}^{\text{SE}} \sim C_0^{\text{SE}} \text{H}_{5/4}(\zeta^{\text{SE}}, x_{\parallel}^{\text{SE}}), \quad (65b)$$

with

$$C_0^{\text{NW}} = e^{i\frac{5\pi}{8}(1-\epsilon)} \left(\frac{\nu}{\omega}\right)^{1/12} \left(\frac{r_c}{2}\right)^{1/4} (G_u U_S + iG_v V_S), \quad (66a)$$

$$C_0^{\text{SE}} = e^{i\epsilon\pi/4} C_0^{\text{NW}}, \quad (66b)$$

and

$$G_u = \frac{F_u}{2\Lambda^{5/12}} = \frac{(\gamma^2 \cos^2 \theta + \sin^2 \theta)}{4(\sin 2\theta)^{1/12} |\gamma^2 - 1|^{1/12} (2\gamma^2 \cos^2 \theta + \sin^2 \theta)^{11/12}}, \quad (67a)$$

$$G_v = \frac{F_v}{2\Lambda^{5/12}} = \frac{\gamma \cos \theta (\gamma^2 \cos^2 \theta + \sin^2 \theta)^{1/2}}{4(\sin 2\theta)^{1/12} |\gamma^2 - 1|^{1/12} (2\gamma^2 \cos^2 \theta + \sin^2 \theta)^{11/12}}, \quad (67b)$$

where $\gamma = 2\Omega/N$ and H_{μ} has been defined in (40-43).

Expressions (65a,b) with (66a,b) mean that the localized beam on the critical line has a velocity amplitude scaling as $(\nu r_c^3 / (\omega x_{\parallel}^5))^{1/12}$ where x_{\parallel} is the distance from the critical point.

Without stratification, we recover the expression obtained for a librating sphere [6, 7, 14] Note that [6] corrected a sign error in the expressions first given in [14]. This is not surprising as this expression was obtained by matching directly the boundary layer solution to the self-similar solution around the critical line. It was then implicitly assumed that nothing was emitted in the NE direction close to the critical point in [14]. The present analysis which gives $D_+ = D_- = 0$ permits to justify this hypothesis.

V. VISCOUS CORRECTIONS TO THE CRITICAL SLOPE SINGULARITY

We have discussed above how an inviscid singularity is generically formed from a critical slope and how this singularity is possibly smoothed by viscosity.

We have seen that the mechanism of generation is essentially inviscid as the singularity properties (strength and amplitude) are directly related the velocity component normal to the boundary. The amplitude of the inviscid waves that are generated is such that their normal velocity matches the normal velocity of the boundary. These waves also possess velocity components that are tangential to the boundary. This tangential velocity is in principle cancelled in a viscous boundary layer. But this process also generates, via Ekman pumping, a normal velocity correction that is responsible of a correction to the emitted inviscid waves. It is the expression of this viscous correction that we want to calculate in this section.

The singular inviscid beam propagating in the North-West direction that is created from the critical point has a velocity component along $\mathbf{e}_{\parallel}^{\text{NW}}$ given by an expression of the form (39). The corresponding transverse velocity v is given by (5). This gives a velocity tangent to the boundary surface S near the critical point which can be expressed as $\mathbf{u}_T = u_t \mathbf{e}_t + v \mathbf{e}_y$ with

$$u_t(\mathbf{x}_S) \sim -u_{\parallel}^{\text{NW}}(\mathbf{x}_S), \quad (68a)$$

$$v(\mathbf{x}_S) \sim \frac{2i\Omega \cos \theta}{\omega} u_{\parallel}^{\text{NW}}(\mathbf{x}_S). \quad (68b)$$

This tangential velocity has to be cancelled in a boundary layer by adding a boundary layer solution satisfying the boundary conditions $u_t^{(0)}(0) = -u_t(\mathbf{x}_S)$ and $v^{(0)}(0) = -v(\mathbf{x}_S)$.

Such a solution has been calculated in the appendix. It is given by (A8). It leads to an expression of the Ekman pumping given by (A14) with

$$\tilde{u}_{t-} \sim u_{\parallel}^{\text{NW}}(\mathbf{x}_S) \quad (69)$$

as obtained from (A17). As both \tilde{u}_{t-} and λ_- are singular, the last two terms of (A14) are now contributing to Ekman pumping. We obtain in terms of the coordinate x_{\perp}^{NE}

$$u_{n\infty} \sim \begin{cases} \frac{-C^{(v)} e^{-i\epsilon\pi(\mu+1/4)}}{|x_{\perp}^{\text{NE}}|^{2\mu+3/2}} & \text{for } x_{\perp}^{\text{NE}} > 0, \\ \frac{C^{(v)} e^{i\epsilon\pi(\mu+1/4)}}{|x_{\perp}^{\text{NE}}|^{2\mu+3/2}} & \text{for } x_{\perp}^{\text{NE}} < 0, \end{cases} \quad (70)$$

with

$$C^{(v)} = E_o \sqrt{\frac{\nu\Lambda}{\omega}} (\mu + 1/4) \left(\frac{2}{r_c}\right)^{1/4} (\sqrt{2r_c} \sin 2\theta)^{2\mu+3/2}, \quad (71)$$

where λ has been defined in (42).

If we apply the formula (37a-e) with

$$C_+ = -C^{(v)} v e^{-i\epsilon\pi(\mu+1/4)}, \quad (72a)$$

$$C_- = C^{(v)} e^{i\epsilon\pi(\mu+1/4)}, \quad (72b)$$

and $\beta = 2\mu + 3/2$, we get

$$D_+^{(v)} = D_-^{(v)} = 0, \quad (73)$$

and

$$E_o^{(v)} = E_o \sqrt{\frac{\nu\Lambda}{\omega}} \left(\frac{r_c}{2}\right)^{1/4} (\mu + 1/4), \quad (74a)$$

$$E_+^{(v)} = -e^{-i\epsilon\pi(\mu+1/4)} E_o^{(v)}, \quad (74b)$$

$$E_-^{(v)} = -e^{i\epsilon\pi(\mu+1/4)} E_o^{(v)}. \quad (74c)$$

This means that the viscous correction associated the critical slope singularity in $|x_{\perp}^{\text{NW}}|^{-\mu}$ gives rise to a stronger singularity in $|x_{\perp}^{\text{NW}}|^{-(\mu+5/4)}$. However, the amplitude has decreased by a factor proportional to $\sqrt{\nu/\omega}$. In the North-West direction, it then gives a viscous self-similar correction of the form

$$u_{\parallel}^{\text{NW}(v)} \sim C^{\text{NW}(v)} H_{\mu+5/4}(x_{\perp}^{\text{NW}}, x_{\parallel}^{\text{NW}}), \quad (75)$$

with

$$C^{\text{NW}(v)} = e^{i\frac{\pi}{2}(\mu+\frac{5}{4})(1-\epsilon)} \left(\frac{\omega}{\nu\Lambda}\right)^{\mu/3+5/12} E_o^{(v)}, \quad (76)$$

which can be written, using (45) and (74a), as

$$C^{\text{NW}(v)} = C^{\text{NW}} e^{i\frac{5\pi}{8}(1-\epsilon)} \left(\frac{\nu\Lambda}{\omega}\right)^{1/12} \left(\frac{r_c}{2}\right)^{1/4} (\mu + 1/4). \quad (77)$$

Similarly, in the SE direction, we get

$$u_{\parallel}^{\text{SE}(v)} \sim C^{\text{SE}(v)} H_{\mu+5/4}(x_{\perp}^{\text{NW}}, x_{\parallel}^{\text{NW}}), \quad (78)$$

with $C^{\text{SE}(v)} = e^{i\epsilon\pi(\mu+1/4)} C^{\text{NW}(v)}$.

In both NW and SE directions, the viscous correction is therefore smaller by a non-dimensional factor of order $(\nu r_c^3 / (\omega x_{\parallel}^5))^{1/12}$ compared to the leading order beam. Interestingly, no viscous correction is generated in the North-East direction.

VI. DISCUSSION

In this paper, we have analysed the generic properties of the singularity generated by critical slopes on waves in a stratified and rotating unbounded fluids. We have shown that this singularity is of inviscid nature and results from a geometric focusing of the normal velocity forcing on the characteristic line tangent to the boundary. By applying the non-viscous boundary conditions on the normal velocity close to the critical point and adequate outwards boundary conditions at infinity, we have been able to obtain relations between coefficients on either side of the singularity lines. Two generic configurations have been analysed: an oscillating translation leading to direct normal velocity forcing, and a tangential boundary oscillation for which the normal velocity forcing results from Ekman pumping. For the first case, we have seen that the velocity singularity is in $|x_{\perp}|^{-1/2}$ but its amplitude cannot be obtained in closed form. For the second case, the velocity singularity is in $|x_{\perp}|^{-5/4}$ and an explicit expression for the amplitude is derived. This stronger singular behaviour for the tangential forcing comes from the singular behaviour of the Ekman pumping close to the critical point.

We have shown how the inviscid singularity can be smoothed by viscosity using the self-similar expression introduced by [16] and [22]. It leads to a thin shear layer of width of order $(\nu x_{\parallel} / \omega)^{1/3}$ and of a velocity amplitude in $(\omega r_c^3 / (\nu x_{\parallel}))^{1/6}$ for the first case and in $(\nu r_c^3 / (\omega x_{\parallel}^5))^{1/12}$ in the second case.

A viscous correction in $\nu^{1/12}$ generated by corrections in the viscous boundary layer has also been calculated for each case. This correction is larger than the next order correction to the self-similar solution which is in $\nu^{1/3}$ [16], and also larger than the viscous correction in $\nu^{1/6}$ obtained when such a solution reflects on a fixed boundary [13].

The analysis has focused on 2D unbounded geometries. The extension to 3D axisymmetric geometry should not be a problem. In that case, there is no global expression for the velocity in terms of a streamfunction, but as long as we are far from the vortex axis, curvature effects are negligible for singular behaviours. Moreover, a self-similar expression describing viscous smoothing also exists in axisymmetric geometries far from the axis [see 7, for instance]. The analysis that has been done for a librating axisymmetric object in a rotating fluid in [14] can then be extended to other types of forcing and in the presence of stratification without difficulty using the results of the present study.

The extension to a closed domain is by contrast a much more complicated issue. In a closed domain, the condition of outward waves from the critical point cannot be used and therefore the analysis a priori breaks down. Depending on the frequency and on the geometry, the characteristics may be periodic, space filling or may converge towards an attractor. Each case is expected to be different for a given forcing. Nevertheless, [6, 7] have demonstrated that, in a spherical shell, the linear periodic solution obtained by librating the inner sphere can still be related in many situations to the critical slope singularity generated from the critical point as if the fluid was unbounded.

Finally, it is worth mentioning that other boundary singularities such as corners or discontinuities could probably be treated by the same approach. The singularity generated by a boundary discontinuity is in particular expected to be in $|x_{\perp}|^{-1}$. It should then give rise to internal shear layers with a velocity amplitude in $\nu^{-1/3}$. It would be interested to provide a complete theory for this case, and extend the present analysis to all the possible singular boundary features.

Appendix A: Ekman pumping

In this section, we discuss the Ekman pumping coming from tangential displacement of a surface. We provide the general expression of the normal velocity obtained close to a critical point due to Ekman pumping.

We consider a 2D surface in the (x, z) plane given by $(x(s), z(s))$ and define the tangent and normal vectors \mathbf{e}_t and \mathbf{e}_n . At the critical point reached for $s = s_c$, the tangent vector \mathbf{e}_t is oriented along with $-\mathbf{e}_{\parallel}^{\text{NW}}$:

$$\mathbf{e}_t(s_c) = -\mathbf{e}_{\parallel}^{\text{NW}} = \cos\theta\mathbf{e}_x - \sin\theta\mathbf{e}_z. \quad (\text{A1})$$

We dimensionalize length and time scales using a characteristic length l_o and the forcing frequency ω . Defining the Ekman number as

$$E = \frac{\nu}{\omega l_o^2}, \quad (\text{A2})$$

the governing equations read

$$-i\omega\mathbf{u} + 2\Omega\mathbf{e}_z \times \mathbf{u} = -\nabla p + b\mathbf{e}_z + E\Delta\mathbf{u}, \quad (\text{A3a})$$

$$-i\omega b + N^2\mathbf{u}\cdot\mathbf{e}_z = 0, \quad (\text{A3b})$$

$$\nabla\cdot\mathbf{u} = 0. \quad (\text{A3c})$$

Defining the tangent and normal velocity components

$$u_t = \frac{x'u + z'w}{\alpha}, \quad u_n = \frac{-z'u + x'w}{\alpha}, \quad (\text{A4})$$

with $\alpha = \sqrt{x'^2 + z'^2}$, where the prime denotes differentiation with respect to s , and introducing the boundary layer scalings

$$(u_t, v, u_n, b, p) = (u_t^{(0)}(s, \eta), v^{(0)}(s, \eta), \sqrt{E}u_n^{(0)}(s, \eta), b^{(0)}(s, \eta), \sqrt{E}p^{(0)}(s, \eta)), \quad (\text{A5})$$

with

$$\eta = \frac{x_n}{\sqrt{E}} \quad (\text{A6})$$

we get from (A3a-c) at leading order

$$-i\omega u_t^{(0)} - 2\Omega \frac{x'}{\alpha} v^{(0)} = \frac{\partial^2 u_t^{(0)}}{\partial \eta^2} + \frac{z'}{\alpha} b^{(0)}, \quad (\text{A7a})$$

$$-i\omega v^{(0)} + 2\Omega \frac{x'}{\alpha} u_t^{(0)} = \frac{\partial^2 v^{(0)}}{\partial \eta^2}, \quad (\text{A7b})$$

$$2\Omega \frac{z'}{\alpha} v^{(0)} = -\frac{\partial p^{(0)}}{\partial \eta} + \frac{x'}{\alpha} b^{(0)}, \quad (\text{A7c})$$

$$-i\omega b^{(0)} + N^2 \frac{z'}{\alpha} u_t^{(0)} = 0, \quad (\text{A7d})$$

$$\frac{1}{\alpha} \frac{\partial u_t^{(0)}}{\partial s} + \frac{\partial u_n^{(0)}}{\partial \eta} = 0. \quad (\text{A7e})$$

Equations (A7a,b,d) form an homogeneous system for the functions $u_t^{(0)}$, $v^{(0)}$ and $b^{(0)}$. The general solution can be expressed as a sum of four exponential functions. Only two of these functions are bounded as $\eta \rightarrow +\infty$, so we get

$$u_t^{(0)} = \tilde{u}_- e^{-\lambda-\eta} + \tilde{u}_+ e^{-\lambda+\eta}, \quad (\text{A8a})$$

$$v^{(0)} = \tilde{v}_- e^{-\lambda-\eta} + \tilde{v}_+ e^{-\lambda+\eta}, \quad (\text{A8b})$$

$$b^{(0)} = \tilde{b}_- e^{-\lambda-\eta} + \tilde{b}_+ e^{-\lambda+\eta}, \quad (\text{A8c})$$

where λ_{\pm} are the solution of positive real part satisfying

$$\lambda_{\pm}^2 = -\frac{i}{\omega} \left(\omega^2 - \frac{N^2 z'^2}{2\alpha^2} \pm \frac{1}{2} \left(\frac{N^4 z'^4}{\alpha^4} + \frac{16\Omega^2 x'^2 \omega^2}{\alpha^2} \right)^{1/2} \right). \quad (\text{A9})$$

Moreover, the amplitudes $\tilde{u}_{t\pm}$, \tilde{v}_{\pm} and \tilde{b}_{\pm} are related between each other by

$$(\lambda_{\pm}^2 + i\omega)\tilde{v}_{\pm} = \frac{2\Omega x'}{\alpha}\tilde{u}_{t\pm}, \quad (\text{A10a})$$

$$i\omega\tilde{b}_{\pm} = \frac{N^2 z'}{\alpha}\tilde{u}_{t\pm}. \quad (\text{A10b})$$

This general solution is not valid up to the critical point where one of the λ_{\pm} vanishes. As shown by [21], the boundary layer becomes larger with a width of order $E^{2/5}$ when we get at a distance of order $E^{1/5}$ from the critical point, and a different ansatz should be used in that region. In the following, we then assume that we are at a distance from the critical point that is large compared to $E^{1/5}$.

We assume that the velocity at the boundary is tangential and given by

$$u_t(\mathbf{x}_S) = U_S(s), \quad (\text{A11a})$$

$$v(\mathbf{x}_S) = V_S(s). \quad (\text{A11b})$$

This gives two additional equations

$$\tilde{u}_{t-} + \tilde{u}_{t+} = U_S, \quad (\text{A12a})$$

$$\tilde{v}_- + \tilde{v}_+ = V_S. \quad (\text{A12b})$$

They can be used together with (A10a) to obtain $\tilde{u}_{t\pm}$

$$\tilde{u}_{t\pm} = \frac{(\lambda_{\pm}^2 + i\omega)U_S - (\lambda_{\mp}^2 + i\omega)(\lambda_{\mp}^2 + i\omega)V_S\alpha/(2\Omega x')}{\lambda_{\pm}^2 - \lambda_{\mp}^2}, \quad (\text{A13})$$

from which we can also deduce \tilde{v}_{\pm} and b_{\pm} using (A10a,b).

The Ekman pumping is given by the value $u_{n\infty}^{(0)}$ of $u_n^{(0)}$ as η goes to infinity. It is obtained from (A7e) using the expression of $u_t^{(0)}$ that we have just obtained and the condition $u_n^{(0)}(\eta = 0) = 0$. The calculation is straightforward. It gives

$$u_{n\infty}^{(0)} = -\frac{\tilde{u}'_{t+}}{\alpha\lambda_+} + \frac{\tilde{u}_{t+}\lambda'_+}{\alpha\lambda_+^2} - \frac{\tilde{u}'_{t-}}{\alpha\lambda_-} + \frac{\tilde{u}_{t-}\lambda'_-}{\alpha\lambda_-^2}. \quad (\text{A14})$$

This is the general expression of Ekman pumping from any surface. We are interested in the behaviour close to a critical point. At such a point s_c ,

$$x'(s_c) = x'_c = \alpha_c \cos \theta, \quad z'(s_c) = z'_c = -\alpha_c \sin \theta, \quad (\text{A15})$$

and one of the two λ_{\pm} vanishes. More precisely, we get close to s_c :

$$\lambda_+^2 \sim \lambda_{+c}^2 = -i\frac{N^2 \sin^2 \theta + 8\Omega^2 \cos^2 \theta}{\omega} = -i\omega - i\frac{4\Omega^2 \cos^2 \theta}{\omega}, \quad (\text{A16a})$$

$$\lambda_-^2 \sim -i\frac{\sin 2\theta(4\Omega^2 - N^2)\omega}{\omega^2 + 4\Omega^2 \cos^2 \theta} \frac{\alpha_c(s - s_c)}{r_c}. \quad (\text{A16b})$$

These behaviours show that the Ekman pumping is dominated by the last term of (A14). Taking into account that (A13) for \tilde{u}_{t-} reduces close to s_c to

$$\tilde{u}_{t-} \sim -i\frac{\omega U_S + i2\Omega \cos \theta V_S}{\lambda_{+c}^2} = \frac{\omega^2 U_S + i2\omega\Omega \cos \theta V_S}{\omega^2 + 4\Omega^2 \cos^2 \theta}, \quad (\text{A17})$$

we get from (A7c) an Ekman pumping that can be written in dimensional form close to the critical point as

$$u_{n\infty} \sim \sqrt{\frac{\nu r_c}{\omega}} \frac{\mp e^{\mp i\pi/4}}{(\alpha_c |s - s_c|)^{3/2}} (\bar{F}_u U_S + i\bar{F}_v V_S), \quad (\text{A18})$$

where \bar{F}_u and \bar{F}_v are functions of θ and $\gamma = 2\Omega/N$ only:

$$\bar{F}_u(\theta, \gamma) = \frac{\gamma^2 \cos^2 \theta + \sin^2 \theta}{2 (\sin 2\theta (2\gamma^2 \cos^2 \theta + \sin^2 \theta) |\gamma^2 - 1|)^{1/2}}, \quad (\text{A19a})$$

$$\bar{F}_v(\theta, \gamma) = \frac{\gamma \cos \theta}{2} \left(\frac{\gamma^2 \cos^2 \theta + \sin^2 \theta}{\sin 2\theta (2\gamma^2 \cos^2 \theta + \sin^2 \theta) |\gamma^2 - 1|} \right)^{1/2}. \quad (\text{A19b})$$

In (A18), the upper sign is taken if $(s - s_c) < 0$, the lower sign if $s - s_c > 0$. We recall that the parameter ϵ is equal to $+1$ if $2\Omega > N$, -1 otherwise.

For $\gamma = 0$ (that is $\Omega = 0$) and $\gamma = \infty$ (that is $N = 0$), we therefore have

$$\bar{F}_u(\theta, 0) = \sqrt{\frac{\tan \theta}{8}}, \quad \bar{F}_v(\theta, 0) = 0, \quad (\text{A20a})$$

$$\bar{F}_u(\theta, \infty) = \bar{F}_v(\theta, \infty) = \frac{1}{4\sqrt{\tan \theta}}, \quad (\text{A20b})$$

which gives for the Ekman pumping

$$u_{n\infty}(\Omega = 0) \sim \sqrt{\frac{\nu r_c}{N}} \frac{\mp e^{\pm i\pi/4}}{(\alpha_c |s - s_c|)^{3/2}} \frac{U_S}{2\sqrt{2}\sqrt{\cos \theta}}, \quad (\text{A21a})$$

$$u_{n\infty}(N = 0) \sim \sqrt{\frac{\nu r_c}{2\Omega}} \frac{\mp e^{\mp i\pi/4}}{(\alpha_c |s - s_c|)^{3/2}} \frac{U_S + iV_S}{4\sqrt{\sin \theta}}. \quad (\text{A21b})$$

-
- [1] J. C. Appleby and D. G. Crighton. Internal gravity waves generated by oscillations of a sphere. *J. Fluid Mech.*, 183: 439–450, 1987.
- [2] P. G. Baines. The reflexion of internal/inertial waves from bumpy surfaces. *J. Fluid Mech.*, 46:273–291, 1971.
- [3] P. G. Baines. The reflexion of internal/inertial waves from bumpy surfaces. Part 2. Split reflexion and diffraction. *J. Fluid Mech.*, 49:113–131, 1971.
- [4] P. Echeverri and T. Peacock. Internal tide generation by arbitrary two-dimensional topography. *J. Fluid Mech.*, 659: 247–266, 2010.
- [5] H. P. Greenspan. *The theory of rotating fluids*. Cambridge University Press, 1968.
- [6] J. He, B. Favier, M. Rieutord, and S. Le Dizès. Internal shear layers in librating spherical shells: the case of periodic characteristic paths. *J. Fluid Mech.*, 939:A3, 2022.
- [7] J. He, B. Favier, M. Rieutord, and S. Le Dizès. Internal shear layers in librating spherical shells: the case of attractors. *J. Fluid Mech.*, 2023. (submitted).
- [8] D. G. Hurley. The generation of internal waves by vibrating elliptic cylinders. Part 1. Inviscid solution. *J. Fluid Mech.*, 351:105–118, 1997.
- [9] D. G. Hurley and G. Keady. The generation of internal waves by vibrating elliptic cylinders. Part 2. Approximate viscous solution. *J. Fluid Mech.*, 351:119–138, 1997.
- [10] R.R. Kerswell. On the internal shear layers spawned by the critical regions in oscillatory Ekman boundary layers. *J. Fluid Mech.*, 298:311–325, 1995.
- [11] S. Kida. Steady flow in a rapidly rotating sphere with weak precession. *J. Fluid Mech.*, 680:150–193, 2011.
- [12] S. Le Dizès. Wave field and zonal flow of a librating disk. *J. Fluid Mech.*, 782:178–208, 2015.
- [13] S. Le Dizès. Reflection of oscillating internal shear layers: nonlinear corrections. *J. Fluid Mech.*, 899:A21, 2020.
- [14] S. Le Dizès and M. Le Bars. Internal shear layers from librating objects. *J. Fluid Mech.*, 826:653–675, 2017.
- [15] N. Machicoane, P.-P. Cortet, B. Voisin, and F. Moisy. Influence of the multipole order of the source on the decay of an inertial wave beam in a rotating fluid. *Phys. Fluids*, 27:066602, 2015.
- [16] D. W. Moore and P. G. Saffman. The structure of free vertical shear layers in a rotating fluid and the motion produced by a slowly rising body. *Phil. Trans. R. Soc. A*, 264:597–634, 1969.
- [17] D. E. Mowbray and B. S. H. Rarity. A theoretical and experimental investigation of the phase configuration of internal waves of small amplitude in a density stratified liquid. *J. Fluid Mech.*, 28:1–16, 1967.
- [18] Note1. [6] corrected a sign error in the expressions first given in [14].
- [19] K. S. Peat. Internal and inertial waves in a viscous rotating stratified fluid. *Appl. Sci. Res*, 33:481–499, 1978.
- [20] F. Pétrélis, S. Llewellyn Smith, and W. R. Young. Tidal conversion at submarine ridge. *J. Phys. Ocean.*, 36:1053–71, 2006.
- [21] P. H. Roberts and K. Stewartson. On the stability of a MacLaurin spheroid of small viscosity. *Astrophys. J.*, 137:777–790, 1963.
- [22] N. H. Thomas and T. N. Stevenson. A similarity solution for viscous internal waves. *J. Fluid Mech.*, 54:495–506, 1972.
- [23] B. Voisin. Limit states of internal wave beams. *J. Fluid Mech.*, 496:243–293, 2003.
- [24] B. Voisin. Near-field internal wave beams in two dimensions. *J. Fluid Mech.*, 900:A3, 2020.
- [25] B. Voisin. Boundary integrals for oscillating bodies in stratified fluids. *J. Fluid Mech.*, 927:A3, 2021.
- [26] I. C. Walton. Viscous shear layers in an oscillating rotating fluid. *Proc. R. Soc. Lond. A*, 344:101–110, 1975.
- [27] H. P. Zhang, B. King, and H. L. Swinney. Experimental study of internal gravity waves generated by supercritical topography. *Phys. Fluids*, 19:096602, 2007.